Analyses of the mechanisms of amplitude modulation of aero-acoustic wind turbine sound

Fischer, Andreas; Aagaard Madsen , Helge; Kragh, Knud Abildgaard; Bertagnolio, Franck

Published in:
Proceedings of EWEA 2014

Publication date:
2014

Document Version
Publisher's PDF, also known as Version of record

Analyses of the mechanisms of amplitude modulation of aero-acoustic wind turbine sound

Andreas Fischer[1], Helge Aagaard Madsen[1], Knud Abildgaard Kragh[1] and Franck Bertagnolio[1]

[1] Department for Wind Energy, Technical University of Denmark, Frederiksborgvej 399, DK-4000 Roskilde

E-mail: asfi@dtu.dk

Abstract. This paper explores the source mechanism which cause amplitude modulation of the emitted sound of a wind turbine at large distances from the turbine, named as other amplitude modulation. Measurements of the fluctuating surface pressure on a 2.3MW wind turbine showed a considerable variation over a blade revolution in the presence of angle of attack variations. If the blade undergoes transient stall, the variation of the surface pressure spectrum was enhanced and shifted to frequencies below 200Hz. The surface pressure spectra could be directly related to the emitted far field sound. These findings give further evidence that transient stall is a main mechanism to cause other amplitude modulation. Wind shear was identified as a critical condition to cause angle of attack variations. Different control strategies to mitigate other amplitude modulation were proposed.

1. Introduction

The noise emitted from wind turbines and wind parks is an important issue for the development of onshore wind energy. The complaints about noise of people living close by wind turbines have become more numerous in the recent years. Today wind farms have to be operated in derated modes to limit noise emission or in extreme cases even to be shut down to avoid the disturbance of neighbours. And for the development of new projects the noise emission is often a limiting factor.

Wind turbine noise is perceived as even more annoying if the amplitude of the emitted sound modulates. A recently published study by RenewableUK [1] distinguishes between two types of amplitude modulation: normal amplitude modulation (NAM) and other amplitude modulation (OAM). NAM is characterised as a swishing sound which is perceived by a ground based observer at a distance of one or two rotor diameter. In this case trailing edge noise of the blade is the main noise source on the rotor. Due to the directivity of trailing edge noise most of the sound is radiated towards the leading edge and the observer hears the swish when the blade moves towards him. The swishing sound is broad band with a frequency band width ranging approximately from 400Hz to 1000 or 2000Hz. Normally this kind of amplitude modulation is not problematic, because at the typical distance between dwellings and wind farms it cannot be perceived.

OAM is described as a thumping sound with high intensity in the low frequency range below 200Hz. It can be perceived in up and down wind direction at a distance of several kilometres away from the turbine. This kind of amplitude is much more a problem, because it is perceived by

neighbours of the wind farm/turbine. The study [1] named transient stall as possible explanation for OAM. But the conclusion were based on theoretical considerations. The present paper delivers experimental evidence that transient stall causes a significant amplitude modulation of the surface pressure close to the trailing edge of the blade which is the source of the emitted sound.
The first section of the paper outlines a full scale wind turbine experiment. In this experiment the surface pressure fluctuations, inflow vector to the blade and the mean pressure distribution were monitored. In the next section, the surface pressure field is related to the emitted far field sound. These result were obtained from an experiment in an anechoic wind tunnel. In the following section wind conditions which lead to the variation of the surface pressure field over a revolution are identified. In the final section control strategies to mitigate OAM are explored.

2. Surface Pressure field on a MW wind turbine

The DAN-AERO MW project was funded by the Danish Energy Research programme EFP-2007 under contract Journal no. 33033-0074. The project was carried out in the period from March 2007 to December 2009 in corporation between DTU Wind Energy and the companies LM Wind Power, Vestas Wind Systems, Siemens Wind Power and DONG Energy. More details of the project are presented in [2].

2.1. Setup of the Field experiment

One blade of the three bladed NEG-Micon NM80 turbine was heavily equipped with measurement sensors. The turbine has a rotor diameter of 80m and the hub height is 57m, the rated power is 2.3MW. The blade contained pressure tabs at radial position r=13m, 19m, 30m and 37m and four five-hole pitot tubes at radial position r=14.5m, 20.3m, 31m and 36m, figure 1(a). At radial position r=37m, microphones to measure the pressure fluctuations were

(a) NM80 turbine (b) Map of the wind farm

Figure 1. The blade of the NM80 turbine equipped with measurement devices and the map of the wind farm in Tjæreborg Enge. NM80: NM80 turbine, WT: wind turbine, MM: meteorological mast.

distributed along the chord. The microphone on the suction side of the blade which was closed to the trailing edge was located at position x/c=0.84.
The turbine was placed in a small wind farm of 8 turbines at Tjæreborg Enge, about 1km away from the west coast of Jutland, Denmark, figure 1(b). A meteorological mast was situated about half way between the two turbines south-west of the NM80. The mast was equipped with cup anemometers and wind vanes at a height of 17m, 28.5m, 41m, 57m, 77m and 93m to

provide wind speed and direction measurements. Additionally there were 3 sonic anemometers at altitude 17m, 57m and 93m. They provided measurements of the three components of the wind vector.
The wind turbine was operated in an rather unusual way in the selected cases. The blades were pitched to a high negative angle ($-4.5°$) to cause transient blade stall. It ran with constant rotational speed 16.23rpm. The wind speed at hub height was rather high, about 12m/s.

2.2. Blade Inflow and Surface Pressure Field
The wind profiles measured as ten minutes average at the meteorological mast for the two examples from September 1st, 2009 are depicted in figure 2. In both examples the wind speed

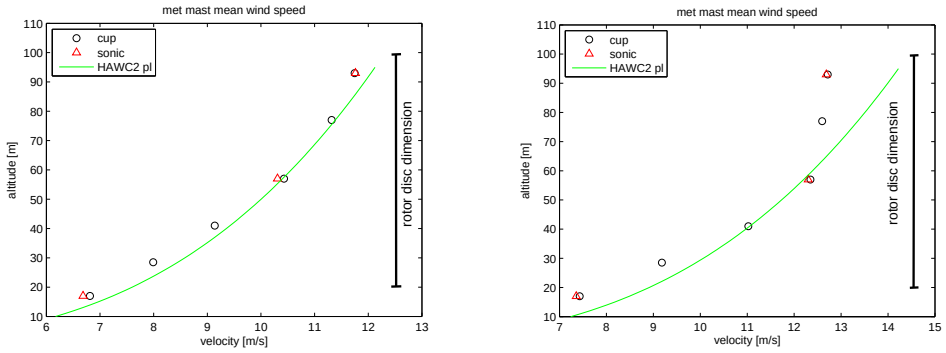

(a) 10:00 (b) 11:40

Figure 2. Wind profile measured at a met mast close to the turbine on Sept. 1st, 2009 (10 minutes average).

at hub height is high and the wind profile can be approximately described by a power law with exponent 0.3. At 11:40 the wind profile is not well described by the power law, because an internal boundary layer had built up. Hence, the shear over the rotor disc is less than for a power law with exponent 0.3, but the wind speed at hub height is higher than in the example at 10:00.
The angle of attack (AoA) for the two cases is presented in figure 3. The AoA was derived from

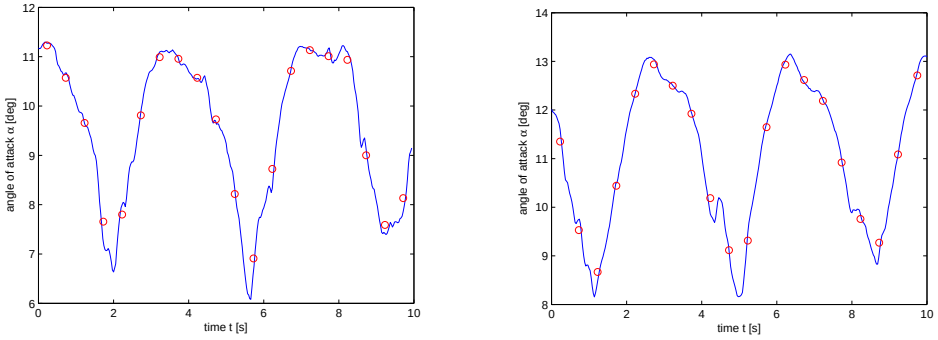

(a) 10:00 (b) 11:40

Figure 3. Measured angle of attack at radial position $r = 31$m. red dots: half second averages.

the measured inflow angle. The inflow angle was corrected for the effects of the bending of the

streamlines due to the presence of the blade. Mathematically it can be described by an extra velocity component proportional to the lift force at the blade.
The difference between the highest and lowest AoA is about 5° in both cases. The variation of the AoA is sinusoidal. It is a function of the azimuth position of the blade. The main difference between the two time series is that at 11:40 higher AoAs are recorded. The pressure distributions, figure 4, indicate the AoA for which the blade stalls. There was a problem with

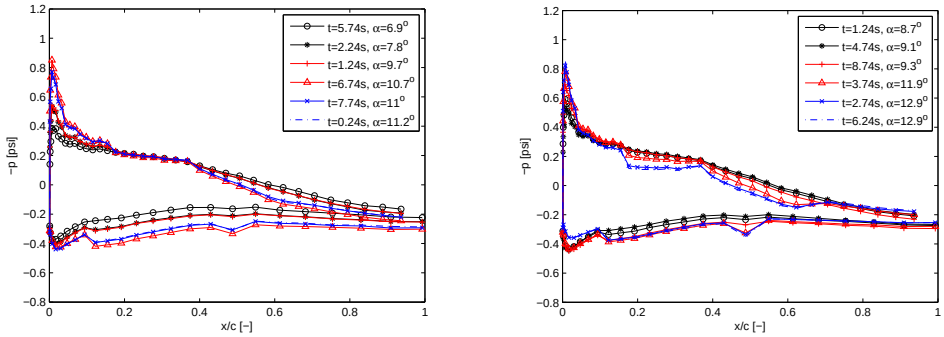

(a) 10:05 (b) 11:48

Figure 4. Surface pressure distribution (mean value) measured on Sept. 1st, 2009.

the pressure sensors and the signal is of low quality. Therefore, the pressure distribution has a ragged appearance and the measurements have a high uncertainty.
The pressure distribution on the suction side indicates stall for the AoA $\alpha = 12.9°$, because it flattens out at x/c=0.6. For the AoA $\alpha = 11.9°$, the blade might be in stall, but due to the low quality of the measurements the interpretation is difficult. For the highest AoA of the time series at 10:00, $\alpha = 11.2°$, there is an adverse pressure gradient on the suction side all the way to the trailing edge. Stall does not occur in this example.
The spectrum of the surface pressure on the suction side at position x/c=0.84 was evaluated for a time interval of 0.5 seconds and is plotted as function of frequency and time in figure 5. There

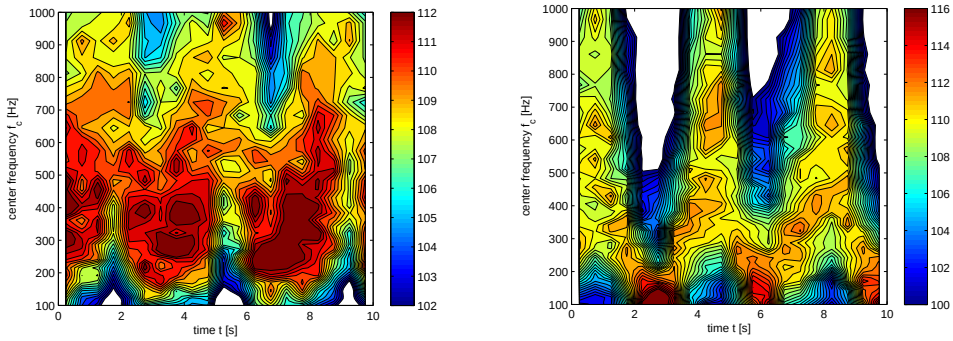

(a) 10:05 (b) 11:48

Figure 5. Narrow band spectra of surface pressure measured on Sept. 1st, 2009. PL in dB(1/12th octave).

is a strong correlation between the spectral energy and the angle of attack. For high AoAs the energy in the low frequency range is high and the energy in the high frequency range is low.

For small AoAs the opposite is the case. The energy in the high frequency range is strongly dampened when sound propagates. Hence, the energy contents in the low frequency range is of concern in this investigation. In the measurement at 10:05 the strongest modulation of the surface pressure over time is found in the frequency range between 200Hz and 500Hz. The peak to peak level is about 8dB. Such a source modulation does probably not lead to OAM, because frequencies above 200Hz are still considerably dampened over such a distance. Additionally, the amplitude modulation of the far field sound is much smaller than the amplitude modulation of the surface pressure on one blade, because the maxima of the source on the three blades are separated in phase by 120°.
In the measurement at 11:48 an amplitude modulation of the surface pressure of 16dB in the frequency range below 150Hz can be detected. Comparing to the analysis above, the maxima of the spectral energy in the low frequency range can be related to blade stall. The source variation is much stronger and more low frequency than in the measurements at 10:05. It is probable that such an amplitude modulation of the surface pressure leads to OAM.

3. The relation between the surface pressure field and the far field sound

In the full scale experiment only surface pressure measurements were available. The relation between the far field sound pressure and the surface pressure needs to be established. In this paper, we use simultaneous measurements of the surface pressure and far field sound made in an acoustic wind tunnel.

3.1. Wind Tunnel Experiment

The measurements presented in this section were made in the acoustic wind tunnel of Virginia Tech University [3] (VTST). The VTST is a classical closed loop wind tunnel. The test section has a cross sectional area of 1.8 times 1.8m and a maximum velocity of 75m/s can be reached. The aerofoil model has a chord length of 0.6m. The Reynolds number range of the experiment was 1 to 2 million. The test section of the VTST is surrounded by an anechoic chamber and the test section walls parallel to the plane of the aerofoil model are made of Kevlar and are transparent for sound, but contain the mean flow, figure 6. Behind the Kevlar walls at a distance

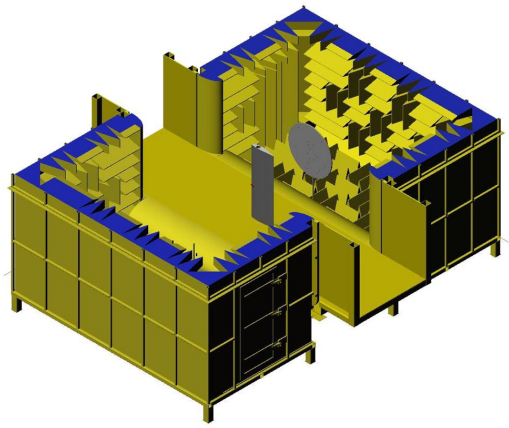

Figure 6. The acoustic test section of the VTST.

of about 1.5m to the aerofoil a microphone array is situated. It consists of 116 microphones and the diameter of the disc is 1.1m.
The aerofoil shape is a NACA64-618 and the model is equipped with microphones connected to the surface of the aerofoil. A tubing system made it possible to place microphones at a distance of only 15mm away from the trailing edge. The pressure field in spanwise and chordwise direction was measured with this surface pressure microphone array. Further details of the experiment are found in [4].

3.2. Noise emission for attached flow conditions

When the flow over the aerofoil is attached, trailing edge noise is the dominant noise source in the experiment and the far field sound pressure can be predicted with the measurements of the surface pressure field and trailing edge noise theory. We chose the trailing edge noise model described in [5] for this task. The comparison between the microphone array measurements of the far field sound pressure and the predictions are shown in figure 7. Detailed measurements of

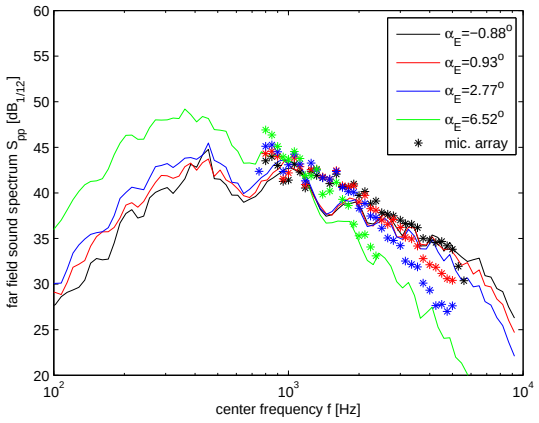

Figure 7. Far field sound pressure spectrum of the NACA64-618 aerofoil measured in the Virginia Tech wind tunnel at Reynolds number $1.5 \cdot 10^6$.

the surface pressure field were only available on the suction side. The pressure side contribution is therefore ignored in the prediction. At high AoAs ($\alpha = 6.52°$), the pressure side contribution is negligible and the prediction is in agreement with the microphone array measurements. For the lower AoAs the pressure side contribution is in the same order of magnitude as the suction side contribution. Therefore the predicted values are up to 3dB to low. It results in slightly lower values than the microphone array measurements.

Overall the agreement between prediction and microphone array is very good and the trends for AoA changes are the same. This proves the direct relation of the measured surface pressure field and the far field sound pressure.

3.3. Noise emission from aerofoils in stall

If the aerofoil is in stall, the mechanism for generating sound is different. Theoretical models for the far field sound prediction exist, for example [6], but have not been implemented yet. For the present study it is sufficient to show a direct correlation between the surface pressure field and the far field sound when the aerofoil is in stall.

In figure 8 the surface pressure spectrum close to the trailing edge and the far field sound pressure spectrum of the aerofoil for Reynolds number 1.9 million are presented. The three different AoAs in figure 8 represent three different flow regimes: attached flow for $\alpha = 6.27°$, the beginning of flow separation close to the trailing edge, $\alpha = 8.23°$, and deep stall with flow separation at the leading edge, $\alpha = 12.21°$. Comparing the attached flow situation with the two stall cases, the far field noise in proportion to the surface pressure increases. But for the two cases in stall the far field sound pressure is in the same proportion to the surface pressure. Therefore we can conclude that the surface pressure on a wind turbine blade can be used to empirically characterise the far field sound even when stall occurs on the blade.

4. Wind conditions and rotor inflow

In section 2 it was shown that the amplitude modulation of the surface pressure is directly linked to AoA variations during a blade revolution. However, the wind turbine operated in an unusual mode. Hence, the measured inflow angle variations are not representative for MW wind turbines

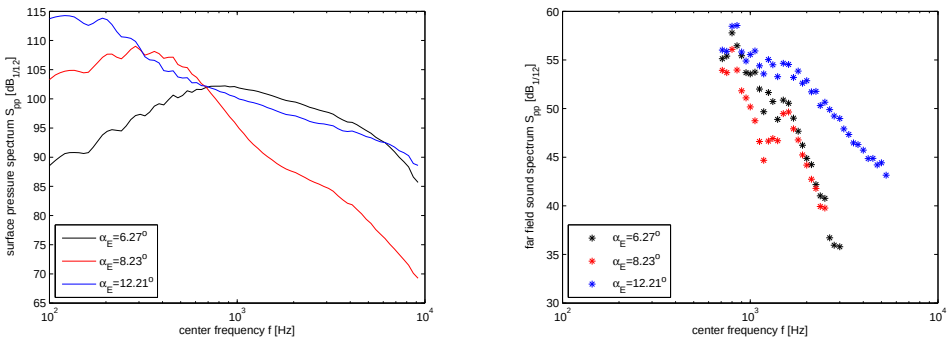

(a) Surface Pressure at x/c=0.975 (b) Far Field Sound Pressure

Figure 8. Pressure spectra for several AoAs of the NACA64-618 aerofoil measured in the Virginia Tech wind tunnel at Reynolds number $1.9 \cdot 10^6$.

in normal operation. In this section flow conditions leading to AoA variations for normal wind turbine operation are identified.

4.1. Setup of second field experiment
Also as part of the DANAERO experiment, a Siemens 3.6MW wind turbine was equipped with a five hole pitot tube to measure the inflow to the blade, figure 9. The pitot tube was located at

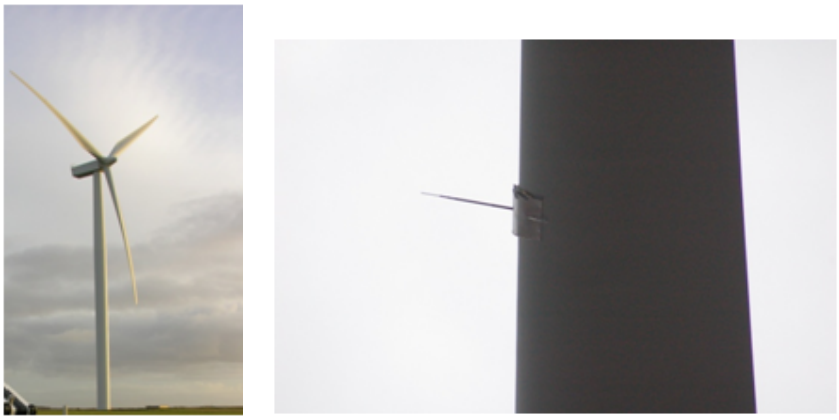

(a) Siemens 3.6 MW Wind Turbine (b) Blade section with pitot tube

Figure 9. The five hole pitot tube mounted at radius 36 m on the blade in a distance of about 0.80 m in front of the leading edge of the blade of a 3.6MW Siemens Wind Turbine.

radial position r=36m, corresponding to 63% of the blade radius. The turbine was located on the Høvsøre test site. On this site there are five stands for MW wind turbines separated by a distance of 300m. Close to each stand a meteorological mast is situated. It measures the wind speed and direction at the altitudes 10m, 40m, 60m, 80m, 100m and 116m.

4.2. Wind shear and inflow angle variations
The wind condition measurements on March 28, 2007 are presented in figure 10(a). On this day very stable conditions during the night led to a strong wind shear. During the day turbulent

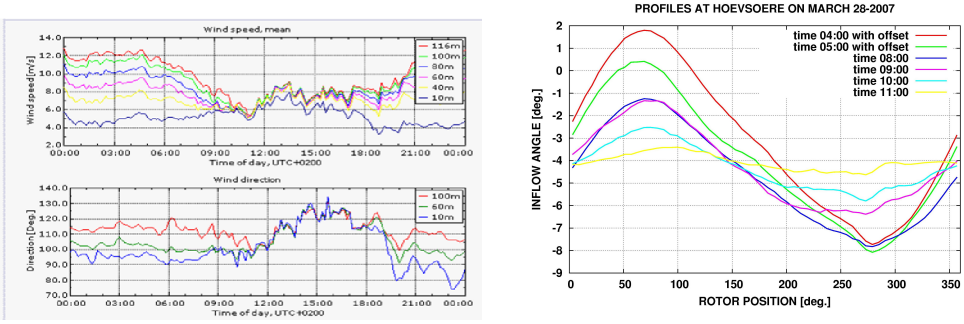

(a) Wind profile (b) Inflow

Figure 10. Measurement of the wind profile and inflow on March 28, 2007.

mixing increased and the velocity profile is close to uniform. The change happened between 4 and 11 o'clock.
The variations of the measured inflow angle, figure 10(b), are directly linked to the wind shear. At 4 o'clock the variations of the inflow angle over a rotation is almost 10°. When the inflow profile becomes uniform at 11 o'clock the variation of the inflow angle is less than 1°.
However, the variations of the measured inflow angle are larger than the variations of the AoA which is more significant for the aerofoil performance. The AoA can be computed from the inflow angle if the lift of the aerofoil section is known. This information was not available in the presented case. Therefore computations with the aeroelastic code HAWC2 [7] were performed and the AoA was converted to the inflow angle and compared to the measurements. To set up the computations the measured shear profiles were linearised, figure 11(a). The computed

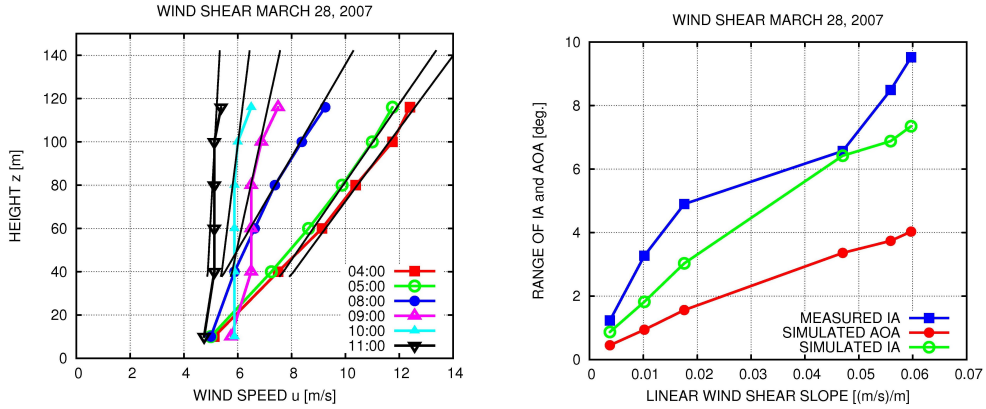

(a) Wind profiles (b) Inflow angle

Figure 11. Wind shear profiles and inflow angle variation as function of linearised shear.

inflow angles match well with the measured ones. The difference might be due to wind veer. The measurements of the met mast show a variation of the wind direction over the rotor disc of about 20°. Wind veer is not modelled in the computation.
However, due to the good agreement of the computed and measured inflow angle we conclude that the AoA variations are predicted correctly by HAWC2. Hence, for the highest measured shear a variation of the AoA over a revolution is about 4°.

5. Control Strategies to mitigate OAM

The control strategies aim on avoiding transient stall. This can be done by operating the blade at lower AoAs and thereby increasing the margin to the stall angle or by decreasing the AoA variations over a revolution. The first strategy can be achieved with a conventional collective pitch controller. For the second option, individual pitch control (IPC) or yaw control is necessary.

5.1. Collective pitch control

The mean AoA at below rated operation can be decreased if the minimum pitch value is increased. The possibilities of decreasing the mean AoA by increasing the minimum pitch angle are investigated by calculating the steady state mean AoA and power production for the NREL 5MW reference turbine [8] using HawcStab2, figure 12. HawcStab2 is an aeroelastic stability

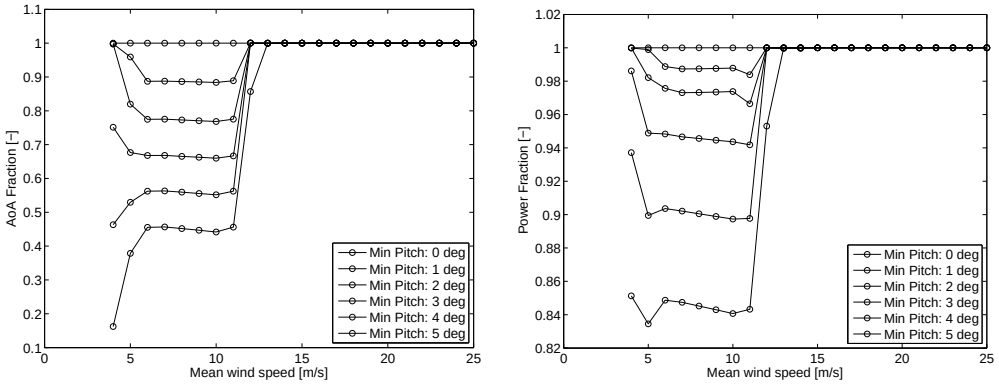

Figure 12. Steady state mean AoA and power production as a function of wind speed when different minimum pitch angles are specified for the variable speed controller. The results are normalised with the mean AoA and power production at a minimum pitch angle of 0°.

simulation tool developed at DTU Wind Energy.
The results have been normalised with the mean AoA and power production a 0° minimum pitch. From this figure it is evident that it is possible to achieve large reductions of the mean AoA and thus operate further away from the stall region. However, it is also seen that these reductions are obtained at the expense of decreased power production.

5.2. Individual pitch control

Simulation for the NREL 5MW reference turbine were performed with the HAWC2 code. An IPC similar to the one described in [9] was implemented in the code. The controller was designed to alleviate azimuthally varying loads, but it is likely to also lower the AoA variations. The results for AoA variations and power production are shown in figure 13. For the uniform inflow, it is seen that the AoA variations are only reduced slightly, because they are small for a uniform inflow. Furthermore, it is seen that for the uniform inflow, the AoA variations are actually increased by the IPC at wind speeds below 8 m/s. This increase is caused by the IPC that seeks to mitigate blade root bending moment variations. At low wind speeds and uniform inflow the blade root bending moment variations are caused by the gravitational loading on the blades. The gravitationally induced blade loads are mitigated by pitch actuation in phase with the AoA variations, which hereby are increased. For the sheared inflow, it is seen that the AoA variations are significantly lowered at both above and below rated wind speeds. The IPC applied in this study is a standard IPC for load mitigation. It is possible that even larger reductions of the AoA variations could be achieved using on-blade inflow measurements and a controller design for AoA variation mitigation.

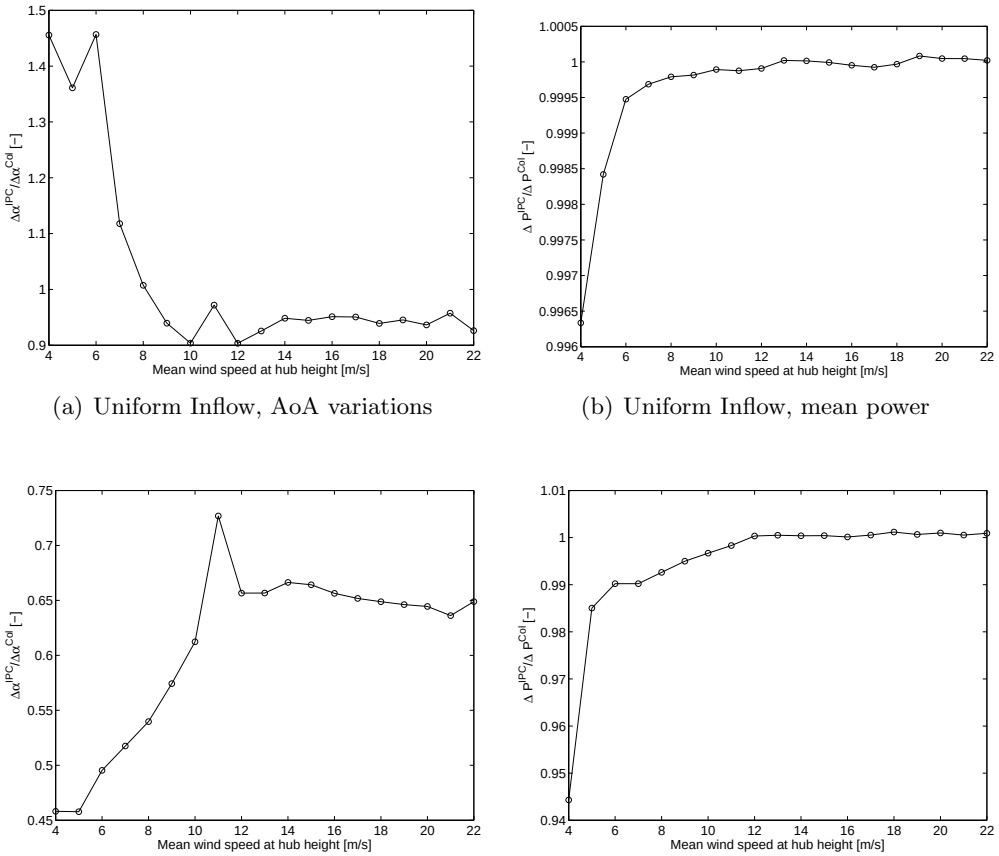

(a) Uniform Inflow, AoA variations

(b) Uniform Inflow, mean power

(c) Sheared Inflow exp=0.5, AoA variations

(d) Sheared Inflow exp=0.5, mean power

Figure 13. Fraction between the magnitude of the AoA variations and fraction between the the mean power for the collective pitch controlled turbine and the individual pitch controlled turbine.

The costs of applying the IPC are increased pitch actuation rates and lowered power output. The greatest power loss is observed for low wind speeds (0.35% for uniform inflow and 5.5% for the sheared inflow). At above rated wind speeds there is no power loss due to the IPC. However, in most cases the power loss is below 1%.

5.3. Yaw control

Yaw control can also be applied for load alleviation [10] by minimising the AoA variation over a revolution. This effect is explored through simulations of the NREL 5MW turbine. Figure 14(a) shows results from a number of simulations where the yaw misalignment angle is varied at one particular wind speed. It is seen that a yaw misalignment angle can be found that minimizes the range of the angle of attack variations. Such an optimum yaw misalignment angle can be found for all wind speeds.

The fraction between the mean power with the optimal yaw misalignment applied and the mean power at 0° yaw misalignment is displayed in figure 14(b). It is seen that the power is actually increased at below rated wind speeds when the optimal yaw misalignment angle is applied. It is surprising that the power is not decreased at below rated wind speeds when the optimal yaw misalignment is applied. However, the increased power might be explained by the asymmetric inflow to the turbine. This phenomena should be investigated further.

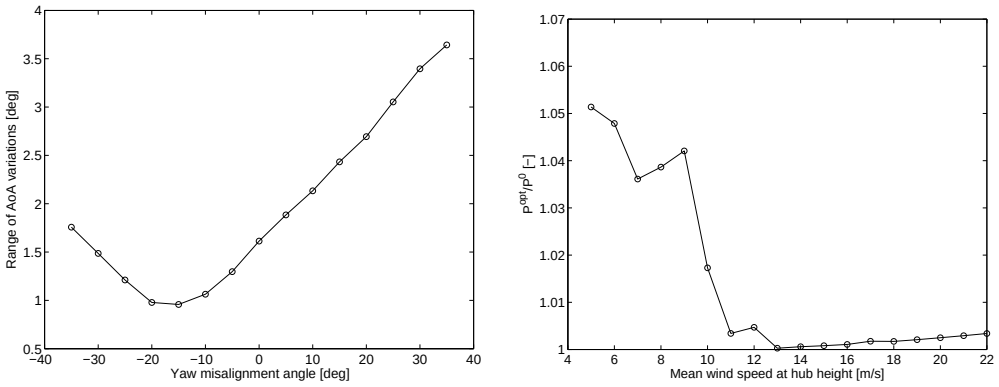

(a) AoA variations, wind speed 8m/s, sheared inflow exp=0.2

(b) Power fraction

Figure 14. Angle of attack variation for specific wind speed and power fraction as function of the mean wind speed.

6. Conclusions

Measurements of the surface pressure on the blade of a MW wind turbine were investigated to identify the mechanisms leading to amplitude modulation of the far field sound. Modulations of the surface pressure level were linked to angle of attack variations over a blade revolution. If the blade was subjected to transient stall, the spectral energy increased strongly in the frequency range below 200Hz. The amplitude modulation of the surface pressure in this frequency range over a blade revolution was about 16dB, double of the value as for cases when the blade was not subjected to transient stall. Hence, the data gives further evidence that other amplitude modulation of the far field sound is caused by transient stall. Measurements in an acoustic wind tunnel validated the method of using surface pressure measurements to characterise the far field sound.

In a second full scale experiment the wind condition which lead to angle of attack variations were investigated. The inflow angle was measured on the blade of a Siemens 3.6MW wind turbine. The variations of the inflow angle could be directly related to wind shear. The angle of attack variations were about 4° for the strongest measured shear. Transient stall only occurs if the blade operates with a small margin to the stall angle. The operational point of the blade is very turbine specific and the conditions leading to transient stall have to be verified for each case. Wind shear seems to be a necessary condition to cause transient stall, but alone it is not sufficient.

Different control strategies to mitigate other amplitude modulation were investigated. With collective pitch control the operation point of the blade can be moved to lower angles of attack and thereby the margin to the stall angle is increased. However, lowering the operational angle of attack leads to significant losses in power. Another control strategy to alleviate other amplitude modulation is to decrease the angle of attack variations over a revolution. It can be achieved by individual pitch control or yaw misalignment control. The power losses with individual pitch control are small, but the pitch actuation rates are increased. For yaw control a significant power loss is expected, but the simulations for a sheared inflow case actually showed an increase of the power production. But it is only a preliminary result and has to be investigated further.

References

[1] Oerlemans S 2011 An explanation for enhanced amplitude modulation of wind turbine noise *Wind Turbine Amplitude Modulation: Research to Improve Understanding as to its Cause*

and Effect, RenewableUK

[2] Madsen H, Bak C, Paulsen U, Gaunaa M, Fuglsang P, Romblad J, Olesen N, Enevoldsen P, Laursen J and Jensen L 2010 The DAN-AERO MW Experiments: Final report Tech. Rep. Risø-R-1726(EN) Risø-DTU, Roskilde, Denmark

[3] Devenport W J, Burdisso R A, Borgoltz A, Ravetta P and Barone M F 2010 Aerodynamic and Acoustic Corrections for a Kevlar-Walled Anechoic Wind Tunnel *Proc. of the 16th AIAA/CEAS Aeracoustics Conference*

[4] Fischer A 2011 *Experimental characterization of airfoil boundary layers for improvement of aeroacoustic and aerodynamic modeling* Ph.D. thesis DTU Technical University of Denmark Roskilde, Denmark

[5] Roger M and Moreau S 2005 *J. Sound Vib.* **286** 477–506

[6] Moreau S, Roger M and Christophe J 2009 Flow Features and Self-Noise of Airfoils Near Stall or in Stall *Proc. of the* 15^{th} *AIAA/CEAS Aeroacoustics Conf.* AIAA Paper 2009-3198 (Miami, FL)

[7] Larsen T J and Hansen A M 2012 How to HAWC2, the users manual Tech. Rep. Risø-R-1597(ver.4-3)(EN) DTU Wind Energy, Roskilde, Denmark

[8] Jonkman J, Butterfield S, Musial W and Scott G 2009 Definition of a 5-MW Reference Wind Turbine for Offshore System Development Tech. Rep. NREL/TP-500-38060 National Renewable Energy Laboratory, Golden, Colorado, USA

[9] Bossanyi E A 2003 *Wind Energy* **6** 119–128 ISSN 1099-1824 URL `http://dx.doi.org/10.1002/we.76`

[10] Kragh K A and Hansen M H 2013 *Wind Energy* n/a–n/a ISSN 1099-1824 URL `http://dx.doi.org/10.1002/we.1612`